

Improving the Predictive Power of Density Functional Theory Calculations

Ann E. Mattsson

Computational Shock and Multiphysics
Sandia National Laboratories, Albuquerque, NM

E-mail: aematts@sandia.gov

Web: <http://www.cs.sandia.gov/~aematts/>
<http://dft.sandia.gov>

IPAM, UCLA, LA, USA
5 September 2013

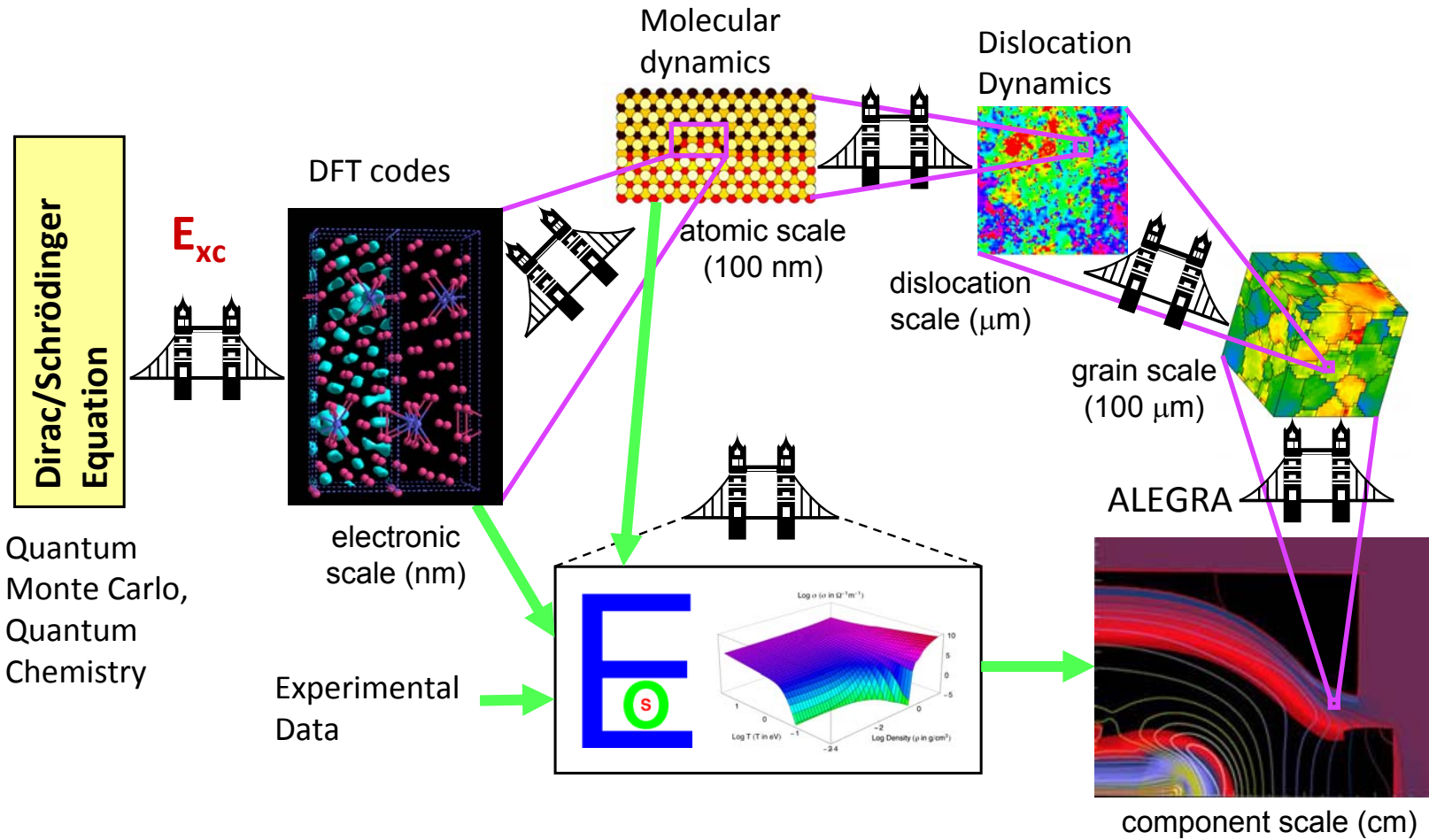
SAND 2013-6597C
SAND 2011-2816P



Sandia National Laboratories is a multi program laboratory managed and operated by Sandia Corporation, a wholly owned subsidiary of Lockheed Martin Corporation, for the U.S. Department of Energy's National Nuclear Security Administration under contract DE-AC04-94AL85000.



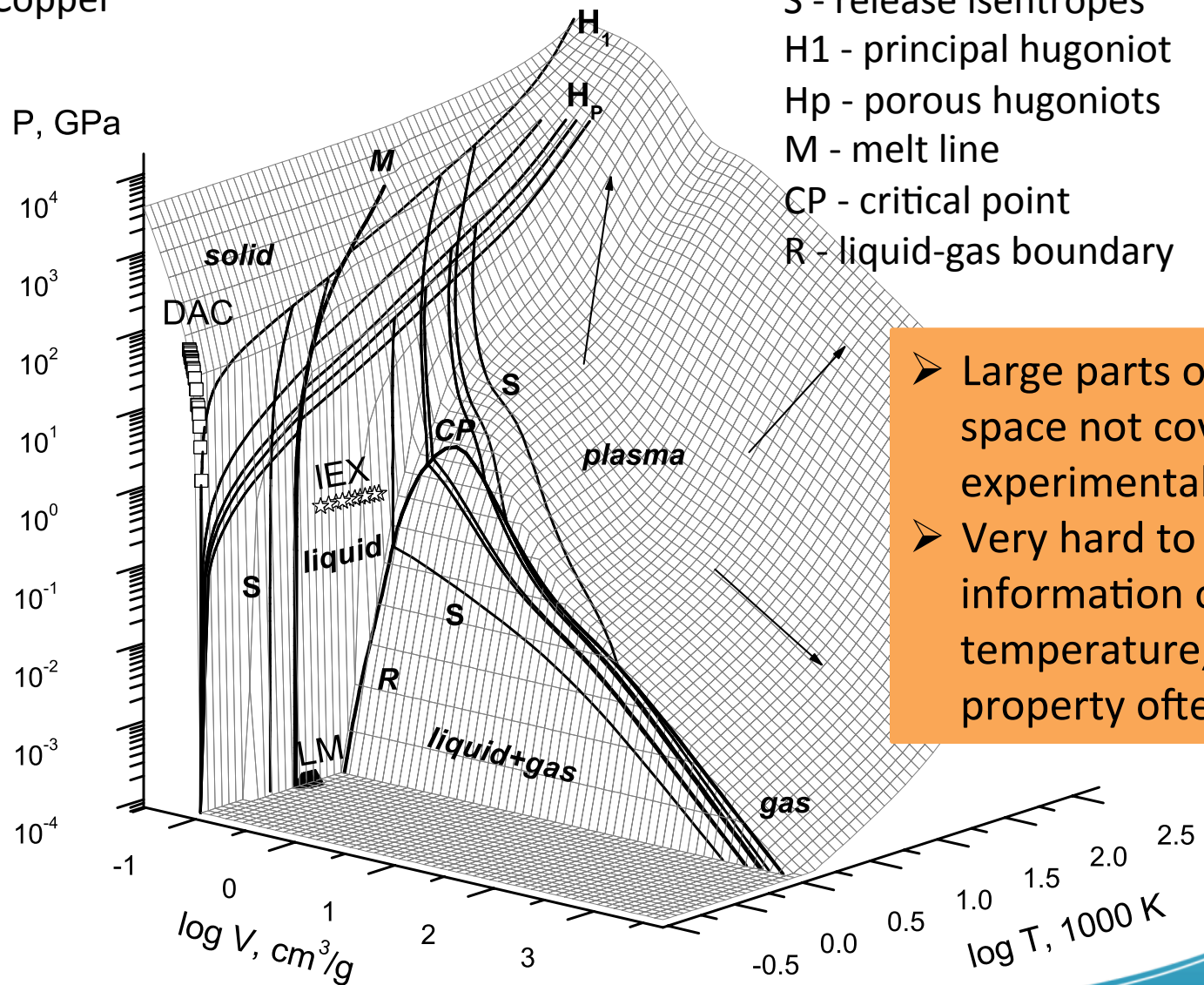
Bridges between Fundamental Law of Nature and Engineering



Equation of State: Example of Material input

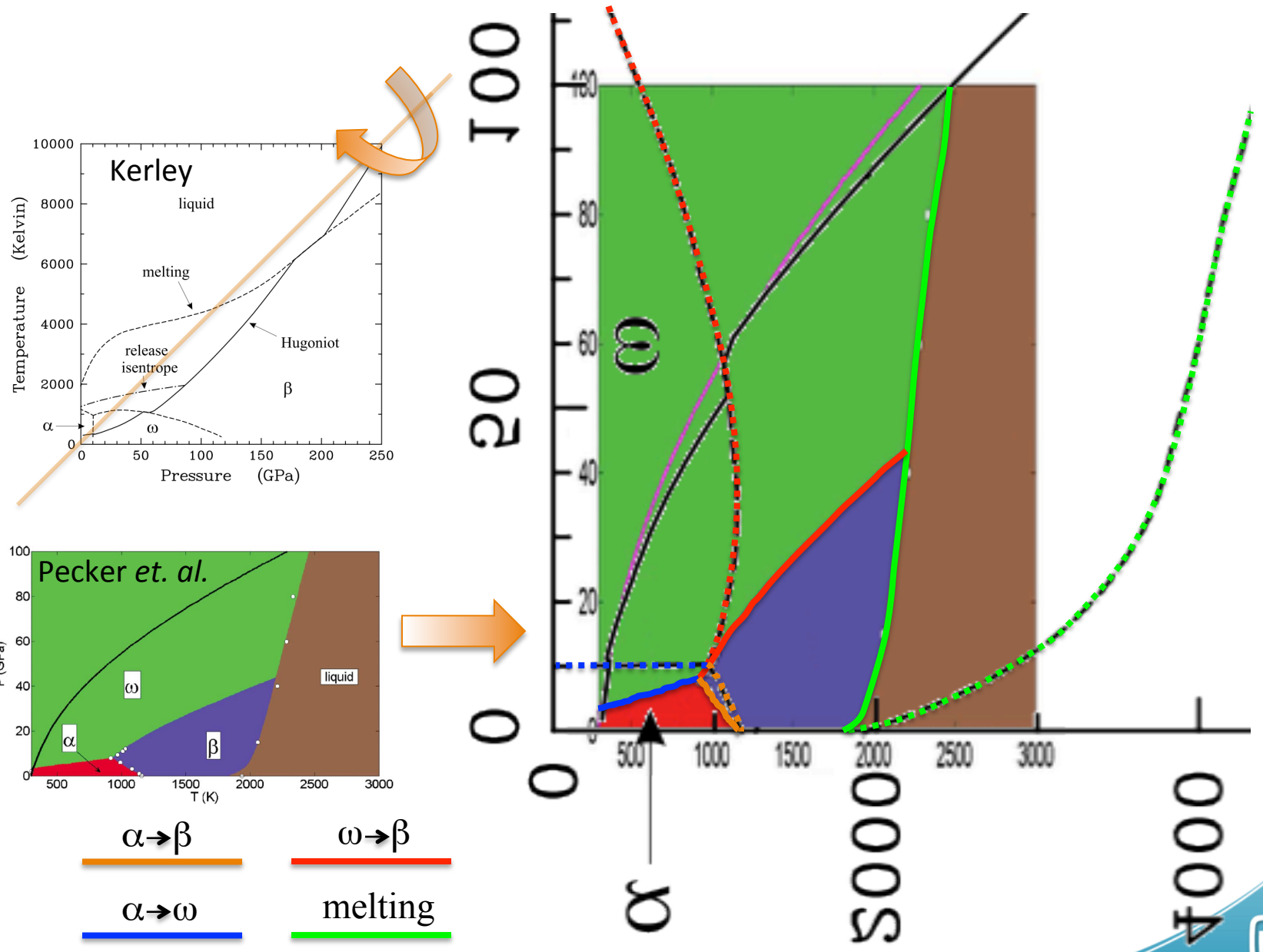
Copper

DAC - diamond anvil cell measurements
IEX - isobaric expansion experiments
S - release isentropes
H₁ - principal hugoniot
H_p - porous hugoniots
M - melt line
CP - critical point
R - liquid-gas boundary

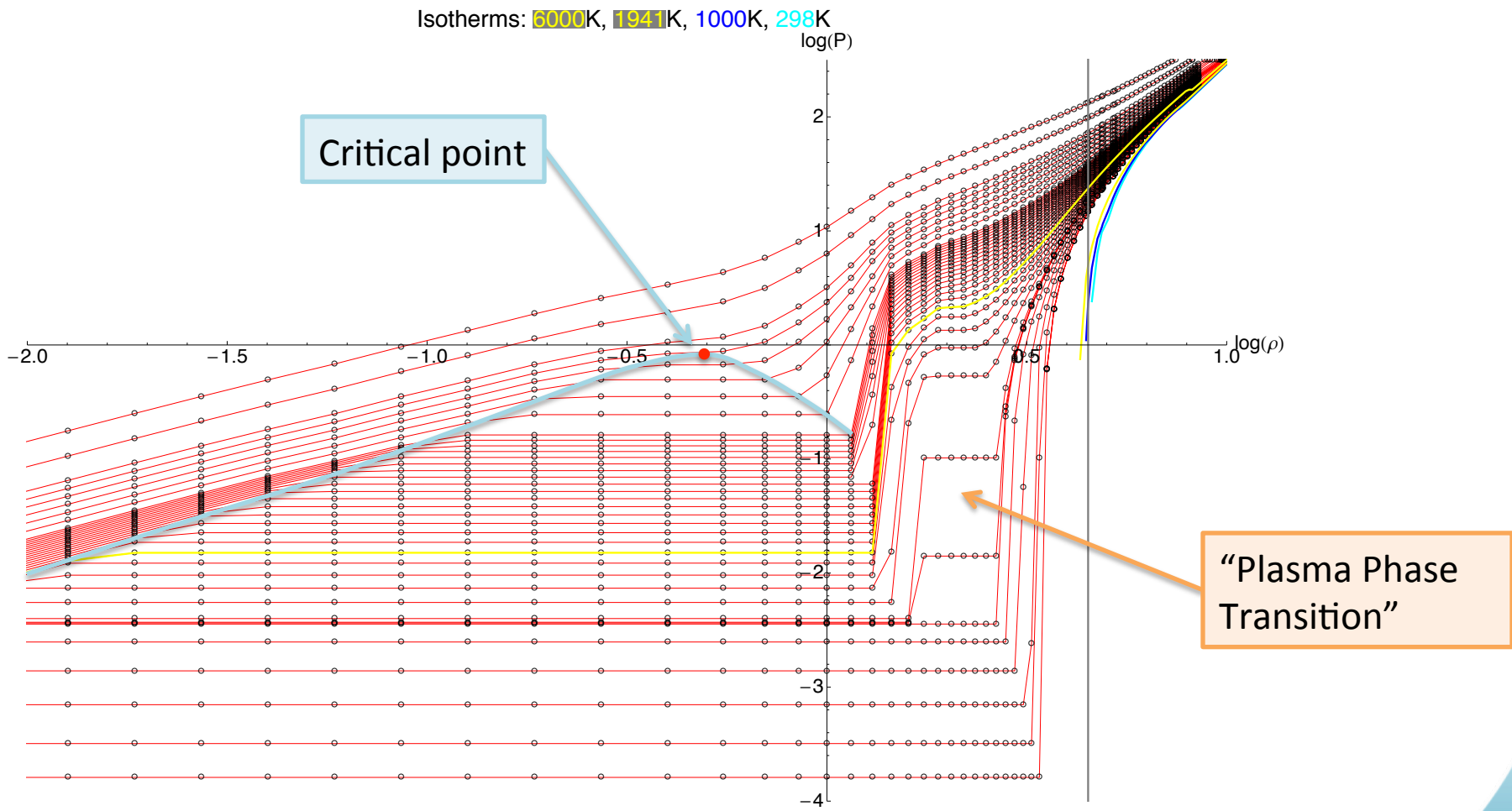


➤ Large parts of parameter space not covered by any experimental technique.
➤ Very hard to get information on temperature, this property often inferred.

Two Ti EOS: Kerley (2003) and Pecker (2005)



More ...

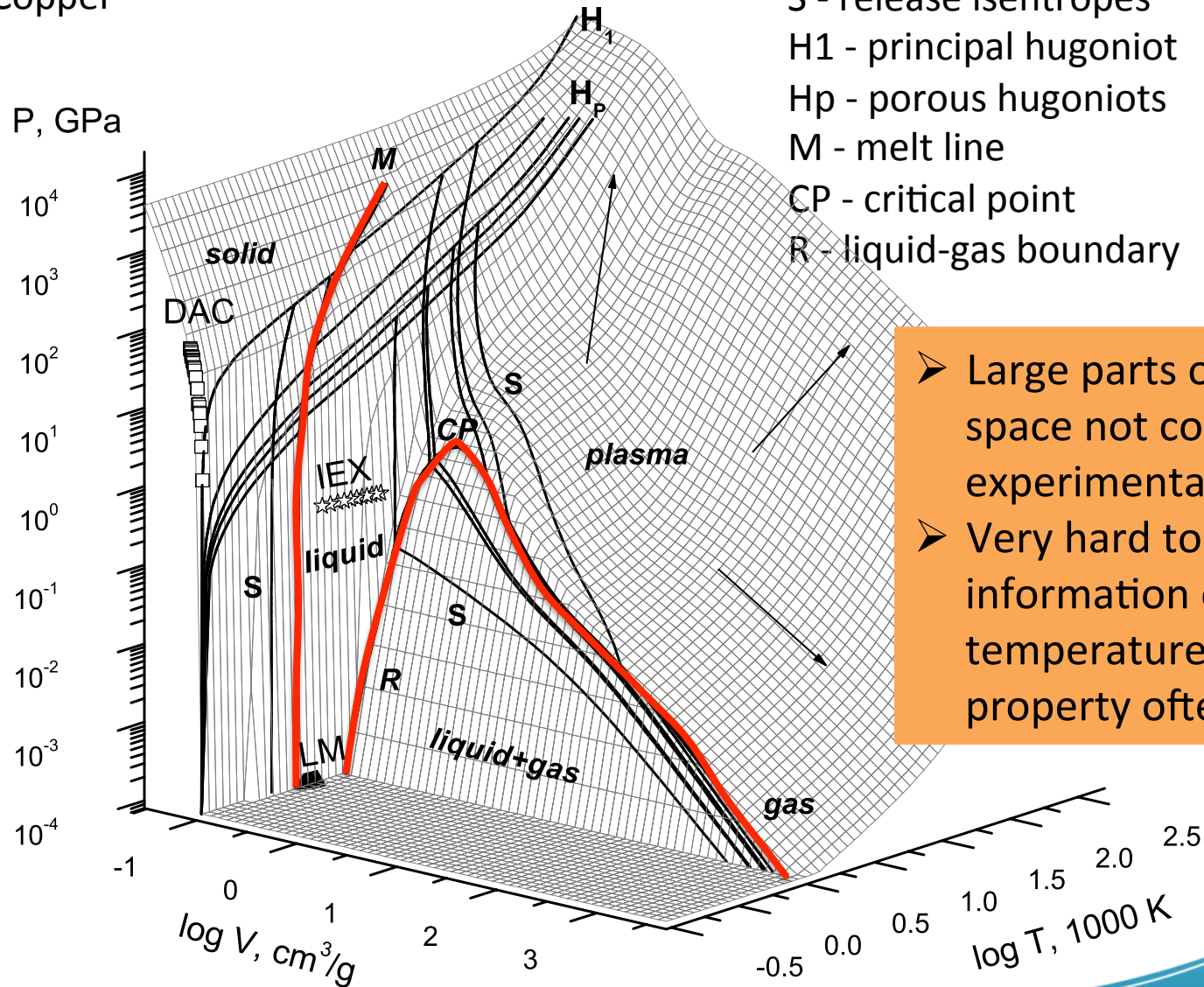


Kerley critical point at 0.5 g/cc and 15500K,
Pecker et al at same density but 9000K.

Equation of State: Example of Material input

Copper

DAC - diamond anvil cell measurements
IEX - isobaric expansion experiments
S - release isentropes
H₁ - principal hugoniot
H_p - porous hugoniots
M - melt line
CP - critical point
R - liquid-gas boundary

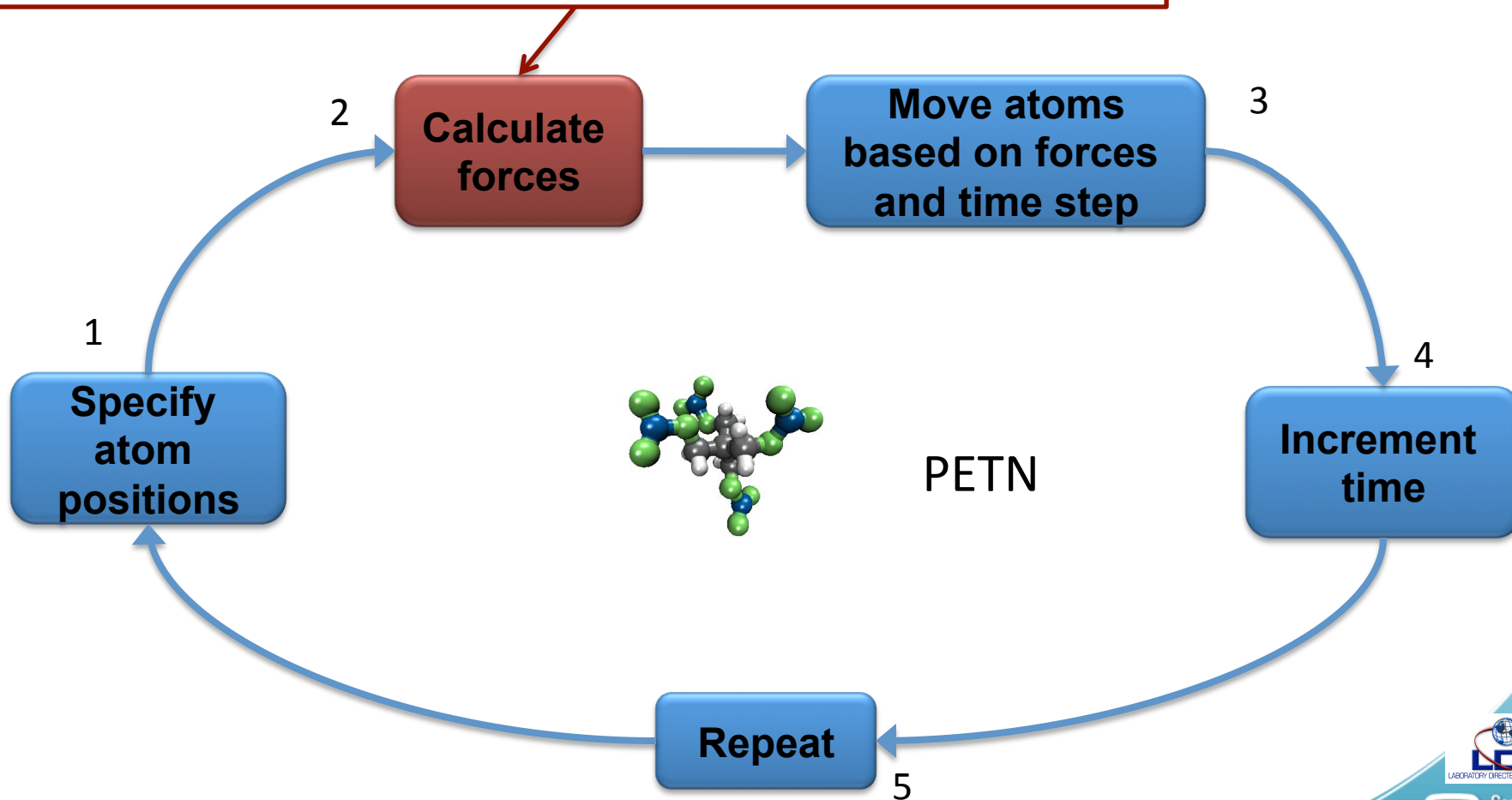


➤ Large parts of parameter space not covered by any experimental technique.
➤ Very hard to get information on temperature, this property often inferred.

Molecular Dynamics

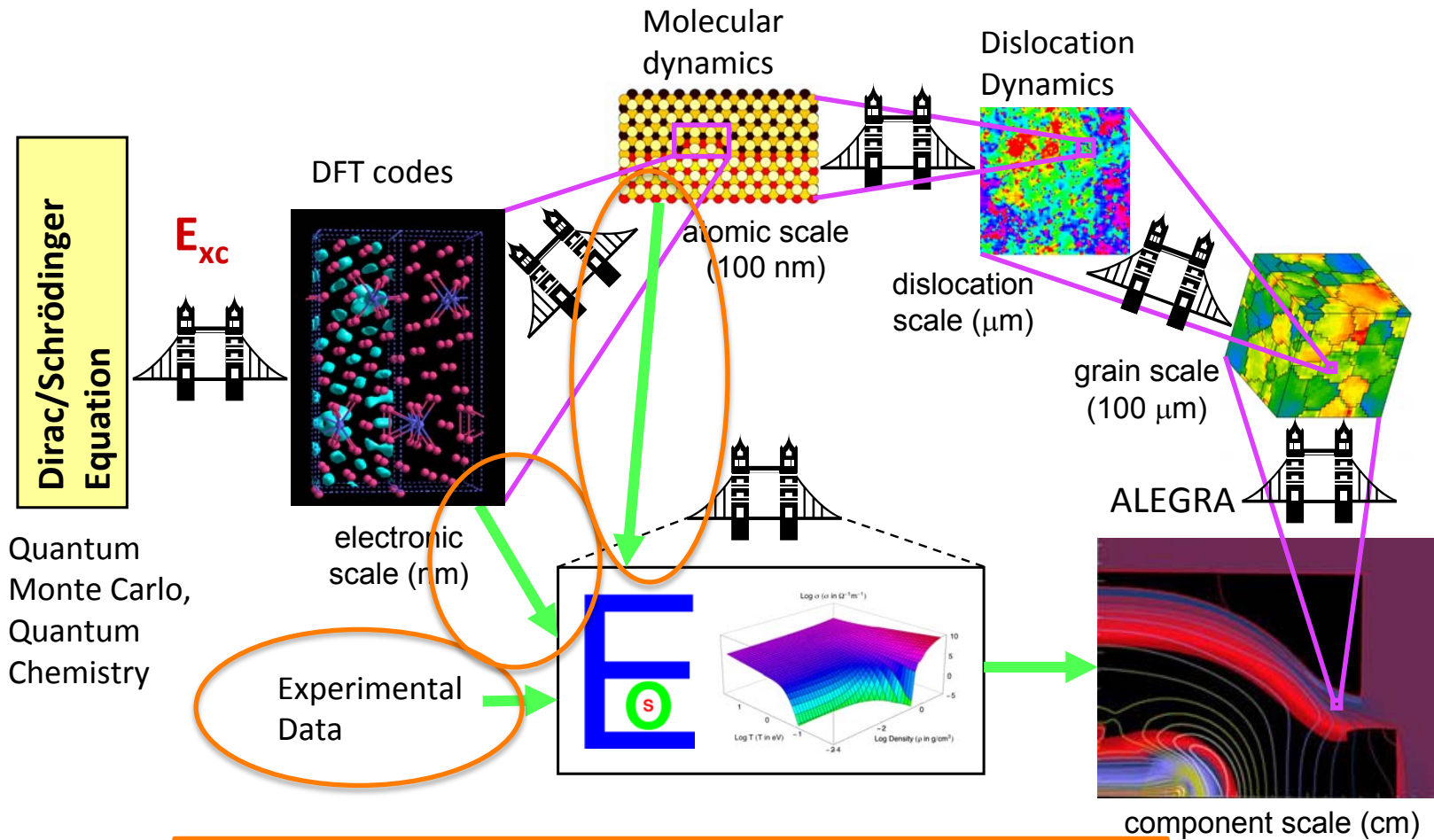
DFT-MD (or a AIMD or QMD): Forces calculated with DFT.

Classical MD: Forces calculated with force fields or potentials.



Adapted from slides by Ryan Wixom, SNL.

Bridges between Fundamental Law of Nature and Engineering

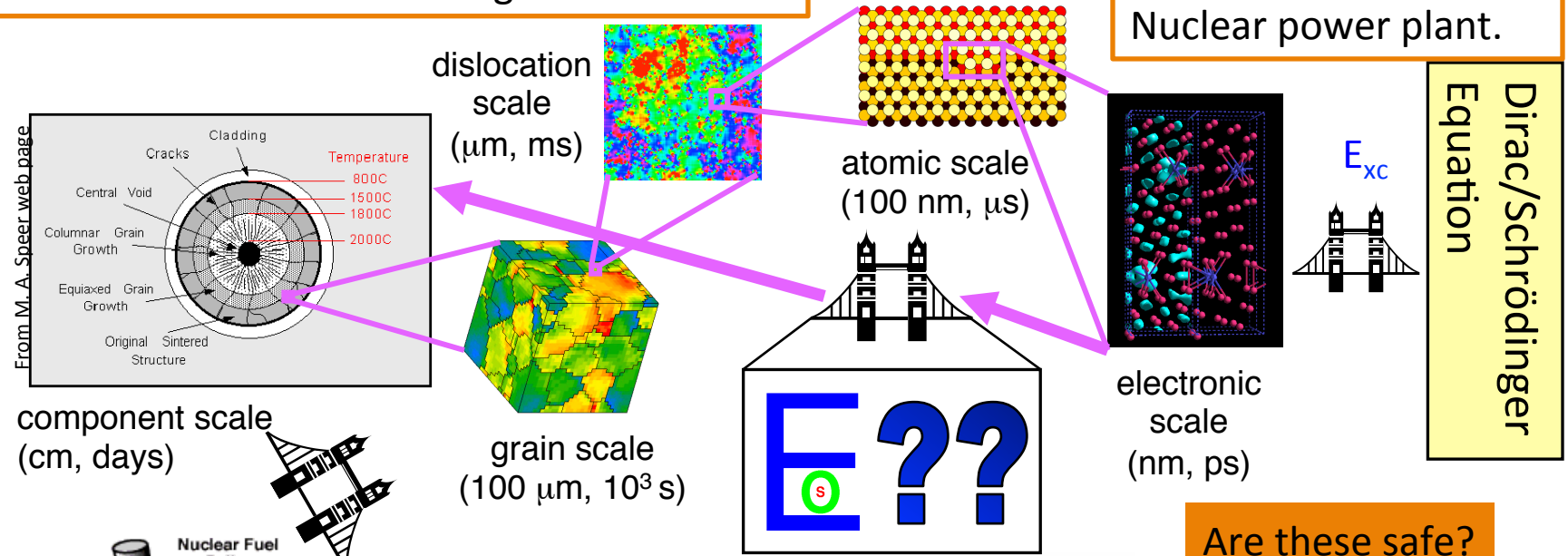


The ability to perform high-fidelity calculations is most important for cases where experiments are impossible, dangerous, and/or prohibitively expensive to perform.

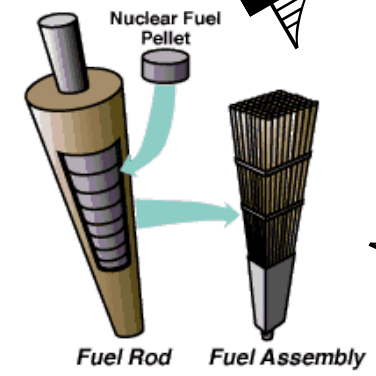
Example: Modeling and simulation of Nuclear Energy related systems

Upscaling needed. In each step, reality that cannot be modeled is resulting in **error bars**.

We cannot solve the Dirac Equation for the Nuclear power plant.

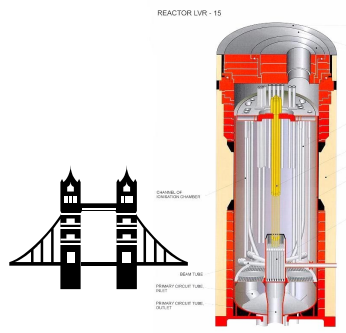
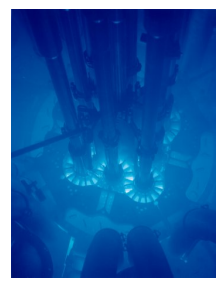


Are these safe?



Courtesy of TXU

system scale (dm, years)



Facility scale (m, many years)

We want to be able to do DFT based calculations for all materials

While DFT is very successful for many materials and many properties, not all materials and properties are equally well treated with DFT. This is the case with, for example, actinides.

We have two problems:

- High atomic numbers means relativistic effects.
- Localized f -electrons means DFT exchange-correlation functionals (including AM05) are not accurate enough.

Relativistic effects

Notably present in Au ($Z=79$), its color, and Hg (liquid).

Similar color effect as in Au already in Cs ($Z=55$).

Indications some effects in Fe ($Z=26$) is due to relativistic effects.

Relativistic Kohn-Sham equations: Functionals

$$\left(c \boldsymbol{\alpha} \cdot \left(\mathbf{p} - \frac{e \mathbf{A}_{eff}}{c} \right) + \begin{pmatrix} I & 0 \\ 0 & I \end{pmatrix} V_{eff}(\mathbf{r}) + \beta m c^2 \right) \psi_n(\mathbf{r}) = E_n \psi_n(\mathbf{r})$$

$$V_{eff}(\mathbf{r}) = -e \left(A_{ext}^0(\mathbf{r}) + \int d^3 r' \frac{J^0(\mathbf{r}')}{|\mathbf{r} - \mathbf{r}'|} + \frac{\delta E_{xc}[J^\mu]}{\delta J^0(\mathbf{r})} \right)$$

$$e \mathbf{A}_{eff}(\mathbf{r}) = -e \left(\mathbf{A}_{ext}(\mathbf{r}) + \int d^3 r' \frac{\mathbf{J}(\mathbf{r}')}{|\mathbf{r} - \mathbf{r}'|} + \frac{\delta E_{xc}[J^\mu]}{\delta \mathbf{J}(\mathbf{r})} \right)$$

$$J^\mu = (J^0, \mathbf{J}) = -e \sum_{-m c^2 < E_n < E_F} (\psi_n^\dagger \psi_n, \psi_n^\dagger \boldsymbol{\alpha} \psi_n)$$

But functionals available from non-relativistic Kohn-Sham theory use spin densities, not currents. The vector potential term is the tricky one, coupling upper and lower components.

From currents to spin densities

Spin density:

$$\mathbf{S} = - \sum_{-mc^2 < E_n < E_F} \psi_n^\dagger \beta \boldsymbol{\Sigma} \psi_n \quad \Sigma_k = \begin{pmatrix} \sigma_k & 0 \\ 0 & \sigma_k \end{pmatrix}$$

Gordon decomposition

$$\mathbf{J} = \mathbf{I} + \mu_B \nabla \times \mathbf{S}$$

$$\mathbf{I} = \frac{e}{2mc} \sum_{-mc^2 < E_n < E_F} \left\{ \psi_n^\dagger \beta \left[\left(\mathbf{p} - \frac{e\mathbf{A}_{eff}}{c} \right) \psi_n \right] + \left[\left(\mathbf{p} - \frac{e\mathbf{A}_{eff}}{c} \right) \psi_n \right]^\dagger \beta \psi_n \right\}$$

Orbital current: Neglecting this gives...

Approximate Dirac for spin density functionals

$$\left(c \boldsymbol{\alpha} \cdot \mathbf{p} + \mu_B \beta \boldsymbol{\Sigma} \cdot \mathbf{B}_{eff} + \begin{pmatrix} I & 0 \\ 0 & I \end{pmatrix} V_{eff}(\mathbf{r}) + \beta mc^2 \right) \psi_n(\mathbf{r}) = E_n \psi_n(\mathbf{r})$$

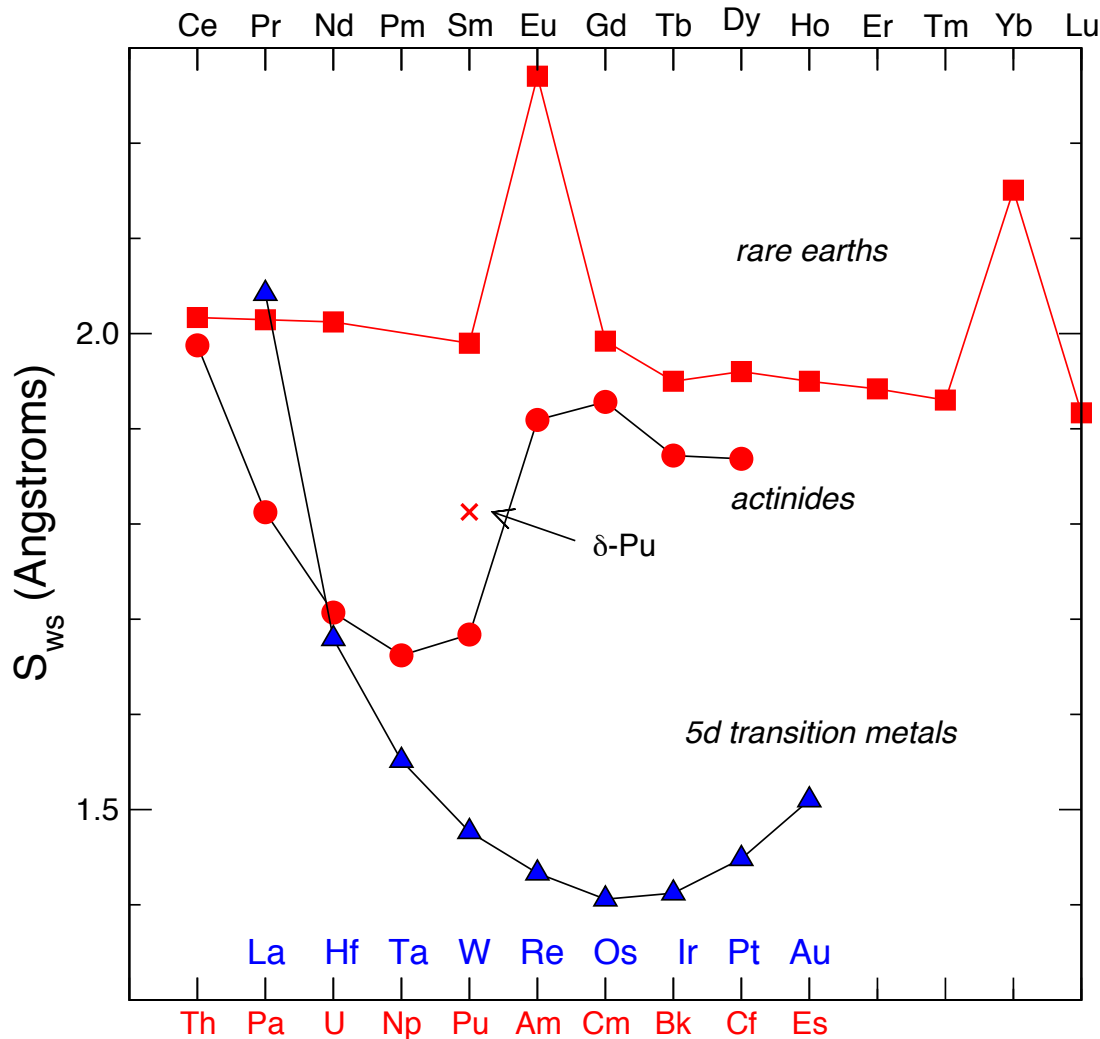
$$V_{eff}(\mathbf{r}) = -e \left(A_{ext}^0(\mathbf{r}) + \int d^3r' \frac{J^0(\mathbf{r}')}{|\mathbf{r} - \mathbf{r}'|} + \frac{\delta E_{xc}[J^\mu]}{\delta J^0(\mathbf{r})} \right)$$

$$\mu_B \mathbf{B}_{eff}(\mathbf{r}) = \left(\mu_B \mathbf{B}_{ext}(\mathbf{r}) + \int d^3r' \frac{\mathbf{M}(\mathbf{r}')}{|\mathbf{r} - \mathbf{r}'|} + \frac{\delta E_{xc}[J^0, \mathbf{M}]}{\delta \mathbf{M}(\mathbf{r})} \right)$$

$$\mathbf{M} = \mu_B \mathbf{S}$$

Now ordinary DFT spin functionals can be used.

Confinement physics



J M Wills and Olle Eriksson, Phys. Rev. B 45, 13879 (1992)

Experimental equilibrium volumes.

✧ LDA/AM05/PBE work reasonably well for 5d transition metals (-2%/0%/+2 %), but, contrary to experiments, give the same parabolic trend for rare earths and actinides.

✧ Dirac treatment does not change this dramatically.

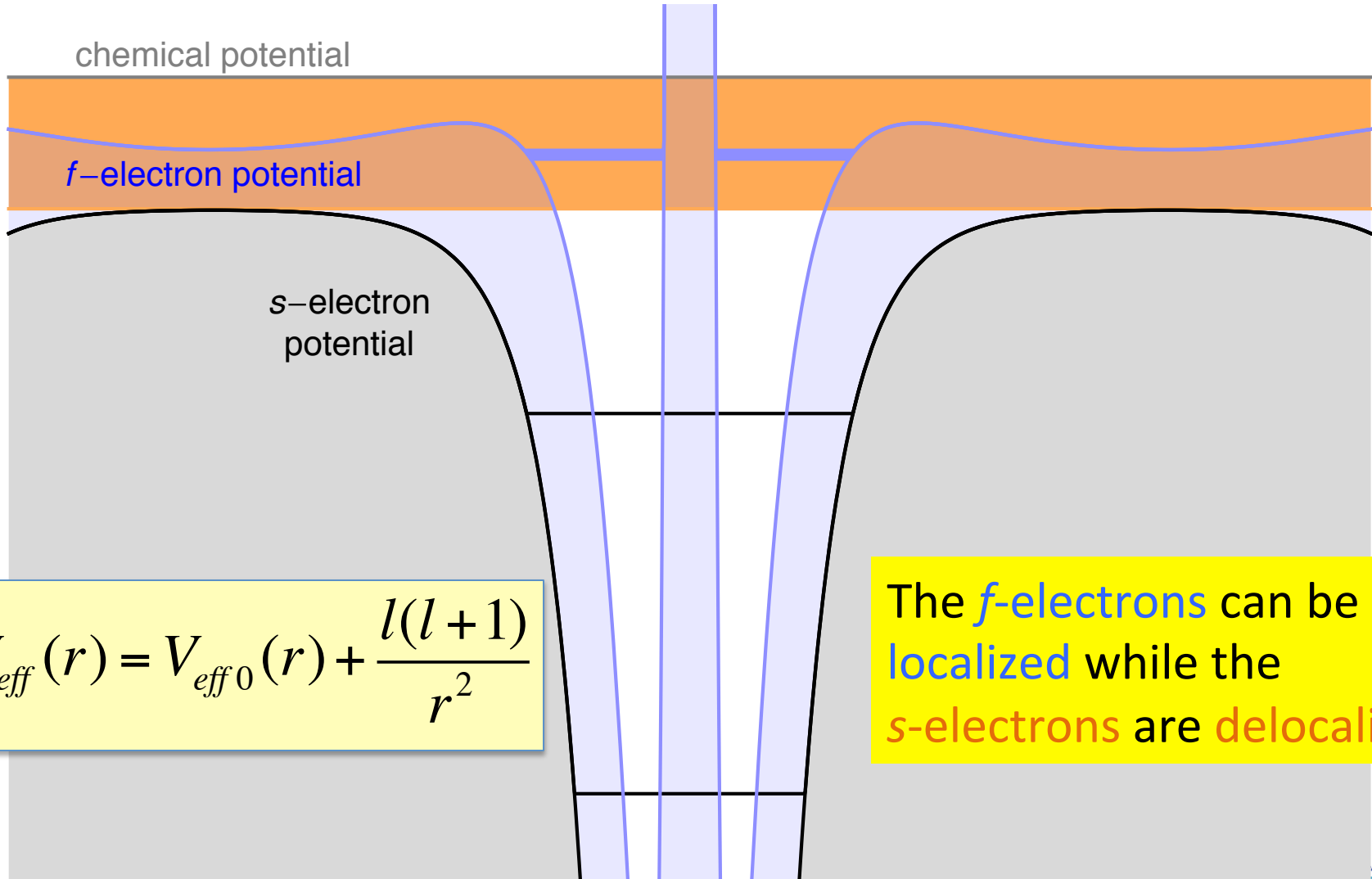
Summary Thorium

TABLE I: Thorium equilibrium volumes in cubic bohrs and bulk moduli in GPa calculated with scalar relativistic, scalar relativistic with variational spin-orbit, and full Dirac methodologies, using AM05¹⁷, PBE², and PW¹⁸ functionals as described in the text. The zero temperature experimental volume, with zero point motion subtracted, is 220.00 bohr³¹³. Reference 13 gives 205.14 for AM05, 218.02 for PBE, and 200.89 for PW.

	V/a ₀ ³			B (GPa)		
	AM05	PBE	PW	AM05	PBE	PW
Scalar Relativistic	204.55	217.36	199.89	58.9	54.5	65.5
Scalar Relativistic+Spin Orbit	189.62	201.21	186.45	74.1	68.6	80.4
Full Dirac	205.98	217.98	201.54	62.4	58.3	68.0

Note: PBE is giving 7% too large volume for gold. Generally underbinding.
 “When PBE gets the right equilibrium volume, you should get suspicious”.
 Seen like an indication that a hybrid functional or exact exchange is needed.
 Confinement physics...

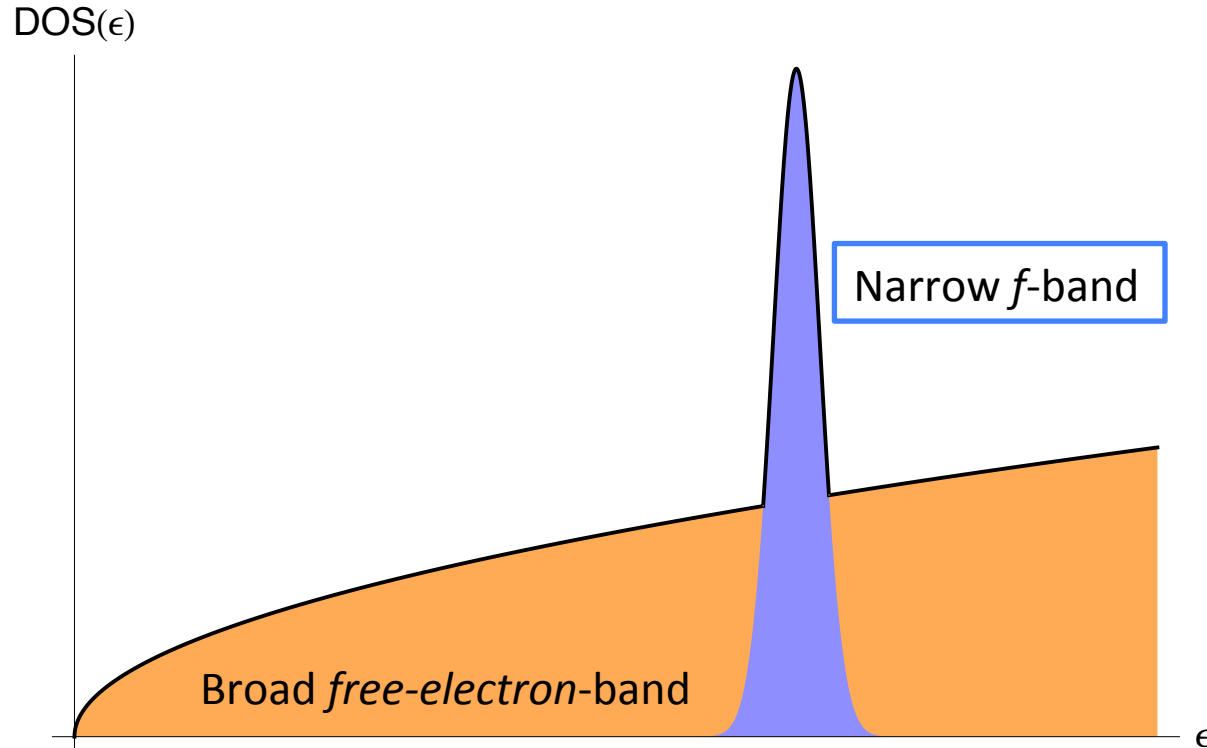
Actinide Physics: Competition between localization and delocalization



$$V_{eff}(r) = V_{eff0}(r) + \frac{l(l+1)}{r^2}$$

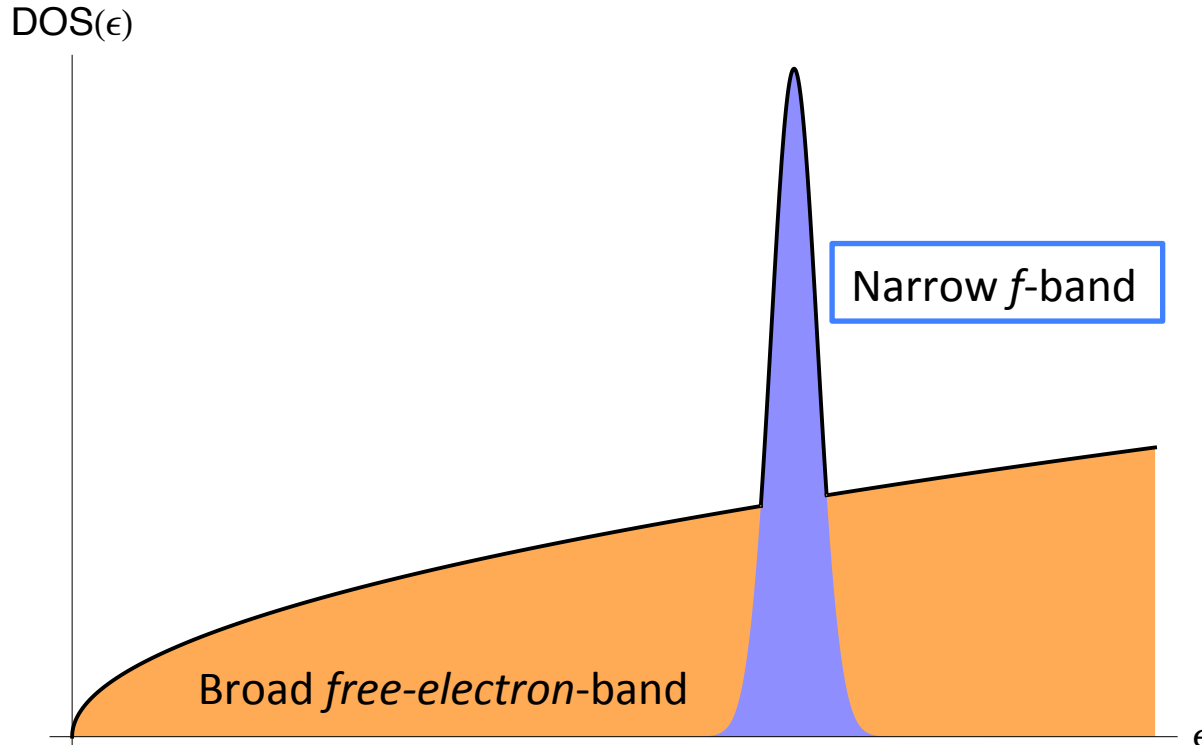
The *f*-electrons can be localized while the *s*-electrons are delocalized.

Actinide Physics: Competition between localization and delocalization



The delocalized electrons in the broad *free-electron* band and the localized electrons in the narrow *f*-electron band are behaving very differently. The interesting physics and chemistry of *f*-electron materials are governed by a competition between these two different pictures.

Actinide Physics: Density Functional Theory



LDA and other functionals based on the uniform electron gas can be expected to work on the broad **free-electron** band.

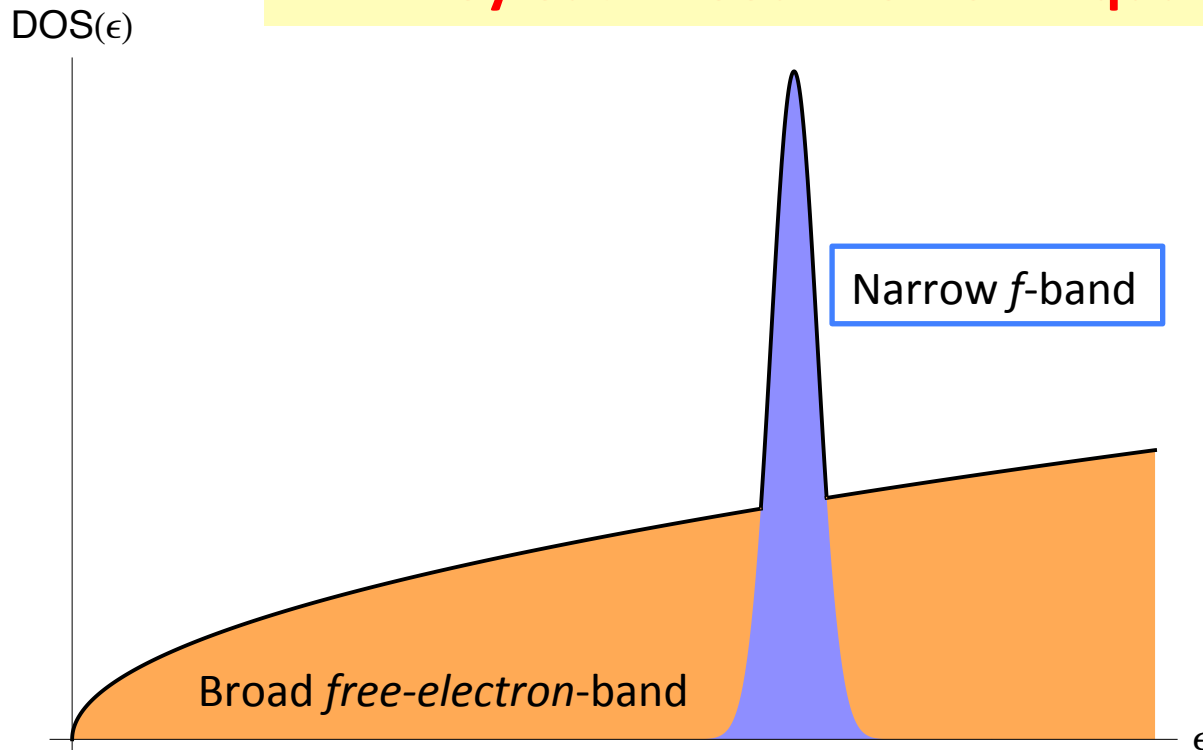
Hybrids and exact exchange are considered needed for **discrete levels**. The Pauli exclusion principle embedded in the **exchange energy** is the main source for describing the fermionic nature of electrons.

Since the physics of actinides is due to the competition between these two types of states, **a functional need to be able to describe the two situations equally well.**

Functionals are applied in real space. How do we take the **discrete level/uniform electron gas** picture to real space?.

Actinide Physics: Electrons are fermions

Electrons are fermions,
they each need their own quantum state.



f-band: 14 *f*-electron states at an ion **all have their own quantum number**. Even with interaction between ions, the *f*-electrons do not need to use a lot of kinetic energy to differentiate between themselves. Compared to the broad free-electron band, **the *f*-band is a collection of discrete levels**.

Free-electron band: The paradigm system describing this situation is the **uniform electron gas**. No potential energy difference gives that they need to differentiate by **different kinetic energies**.

Electron localization function (ELF)

A.D. Becke and K. E. Edgecombe, J. Chem. Phys. **92**, 5397 (1990)

$$ELF = \frac{1}{1 + (D/D_h)^2}$$

$$D = \tau - \frac{1}{8} \frac{|\nabla n|^2}{n}$$

$$D_h = \frac{3}{10} (3\pi^2)^{2/3} n^{5/3}$$

τ : kinetic energy density

n : electron density

D : kinetic energy excess with respect to a **blue gas**.

D_h : kinetic energy of a **uniform electron gas**.

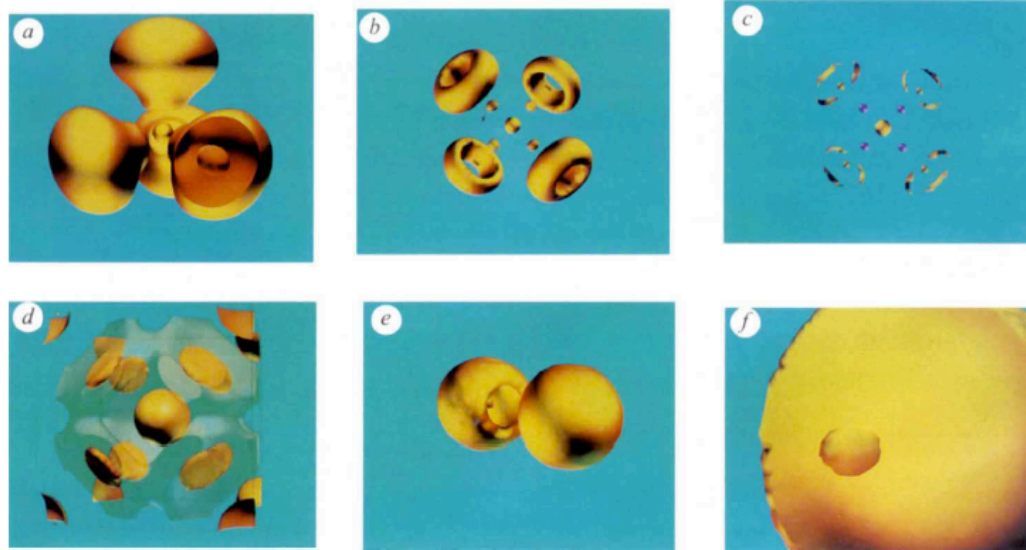


FIG. 1. Localization domains of CF_4 (a-c), Li (d), LiF (e) and LiH (f). a-c, Reduction of the localization domains of CF_4 . Below $ELF = 0.37$ (where ELF is the localization function; see text) there are six localization domains: five core and one valence. The bifurcation at $ELF = 0.37$ splits the common valence domain into four atomic ones. The $ELF = 0.75$ map (a) shows the carbon core surrounded by the four fluorine valence domains; the front cutting plane has been chosen so that a fluorine core domain can be seen. The bonding attractors are responsible for the bulges towards the carbon centre. A further bifurcation occurs at $ELF = 0.78$, giving rise to bonding point attractors and non-bonding ring attractor domains as shown in b ($ELF = 0.85$). Each ring is itself resolved into three non-bonding point attractors for $ELF > 0.883$. In c, the bonding attractors at which $ELF = 0.879$ are represented by purple spheres because the bounding isosurface 0.885 only encapsulates the core and non-bonding attractors. b.c.c. lithium: the core and bonding attractors are located at the 8a (centre and vertices of the cubic lattice) and 8c

(midpoints between the centre and the vertices) positions respectively. Their domains are bounded by the $ELF = 0.625$ isosurfaces, and the $ELF = 0.575$ isosurface forms a network of channels connecting the bonding attractors. These bonding attractors are unsaturated because there are eight per cell sharing two valence electrons. For LiF e, the localization domains shown are bounded by the $ELF = 0.84$ isosurface. The fluorine valence domain (which is almost spherical at lower ELF values) shows a hole in front of the lithium core; increasing the threshold leads to a single attractor lying on the internuclear axis on the side of the fluorine core that is away from the lithium. The $ELF = 0.999$ isosurfaces of LiH (f) encapsulate, on the one hand, the lithium core and, on the other hand, a very large area which extends, in principle, to infinity. The calculation of the grid points has been limited to a box of dimensions $7 \times 7 \times a.u.$, therefore only one face of the largest domain can be seen. The roughness of the surface is due to interpolation limitations and a density cutoff.

B. Silvi and A. Savin, Nature **371**, 683 (1994)

ELF \approx 1/2: uniform electron gas like

ELF \approx 1: strong localization, discrete levels

ELF \approx 0: Classically forbidden region

Subsystem Functional Scheme:

$$E_{xc} = \int_V n(\vec{r}) \varepsilon_{xc}(\vec{r};[n]) dV$$

Dividing V into sub-regions where different subsystem functionals apply

Specialized functionals in different subsystems

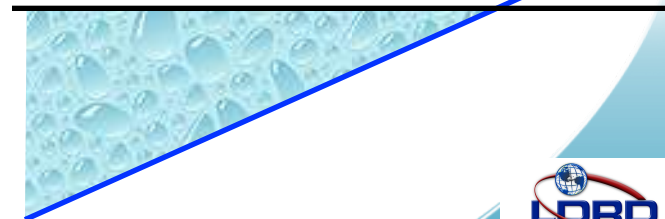


Interior physics:
Uniform electron gas



Interpolation
Index:
ELF

Surface physics:
Airy Gas



LDA and Ceperly-Alder

Ceperly and Alder, PRL 45, 566 (1980).

Quantum Monte Carlo calculations of the ground-state energy of uniform electron gases (model systems) of different densities.

Most correlation functionals in use today are based on their data.

ALL LDA correlation functionals in common use are based on (fitted to) their data.

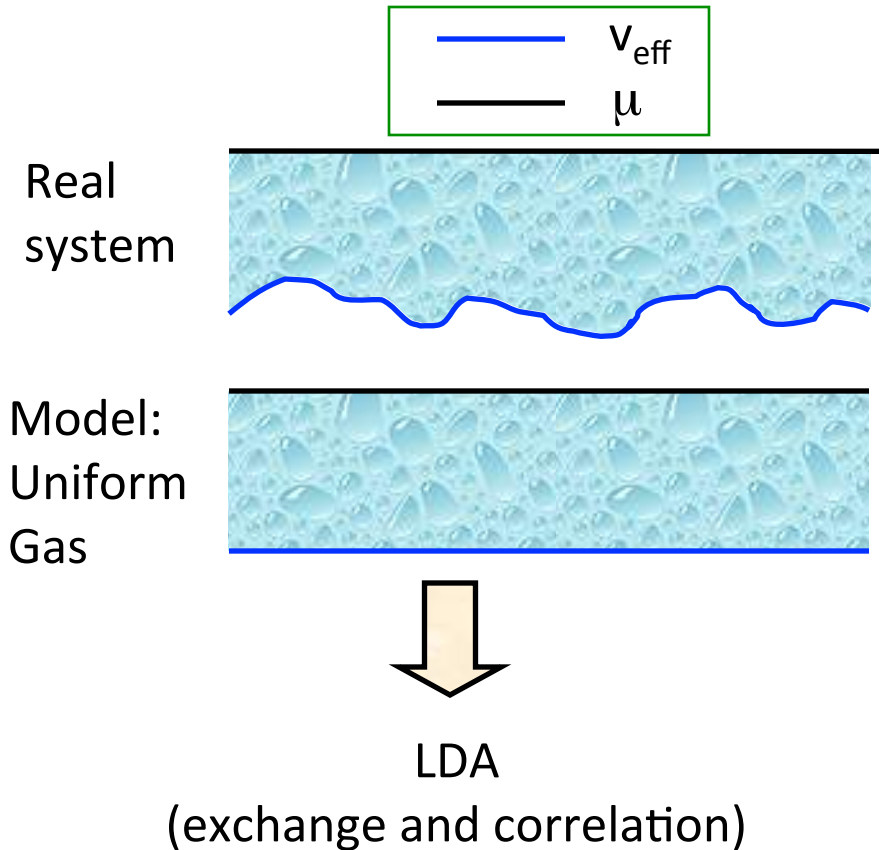
(Before 1980, for example, Wigner correlation was used)

Total energy – energies from known formulas = Exchange-correlation energy.

From SE

From DFT

The LDA functional



Assume each point in the real system contribute the amount of exchange-correlation energy as would a uniform electron gas with the same density.

Obviously exact for the uniform electron gas.

Basic concept and first explicit LDA published in 1965 (Kohn and Sham).

Subsystem functionals

From
general purpose functionals
to
specialized functionals

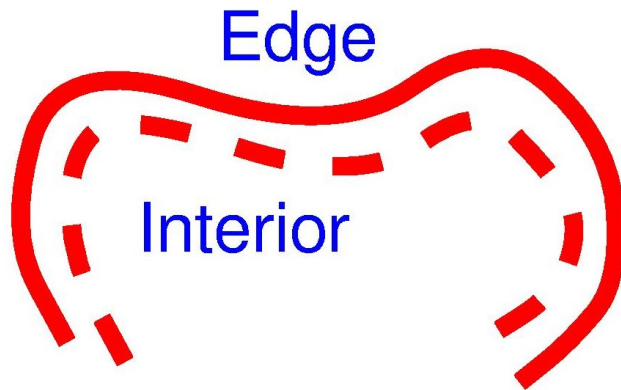
$$E_{xc} = \int_V n(\mathbf{r}) \epsilon_{xc}(\mathbf{r}; [n]) dV$$

Divide integration over V
into integrations over subsystems

Use specialized functionals
in the different subsystems

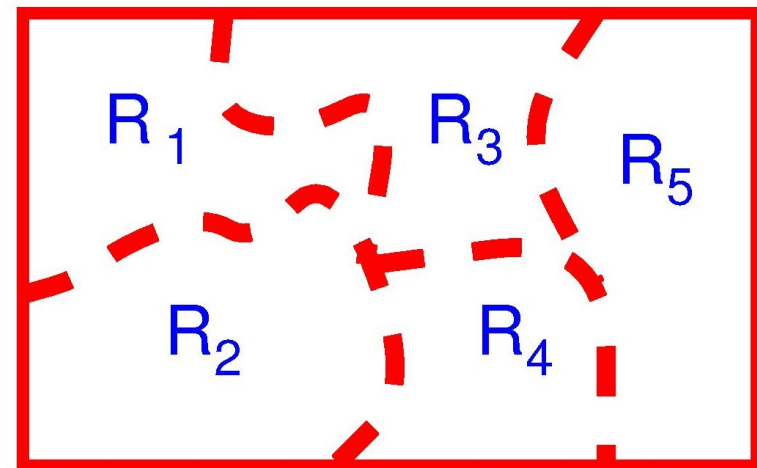
Subsystem functionals

Original Kohn and Mattsson approach



Kohn, Mattsson PRL 81, 3487 (1998)

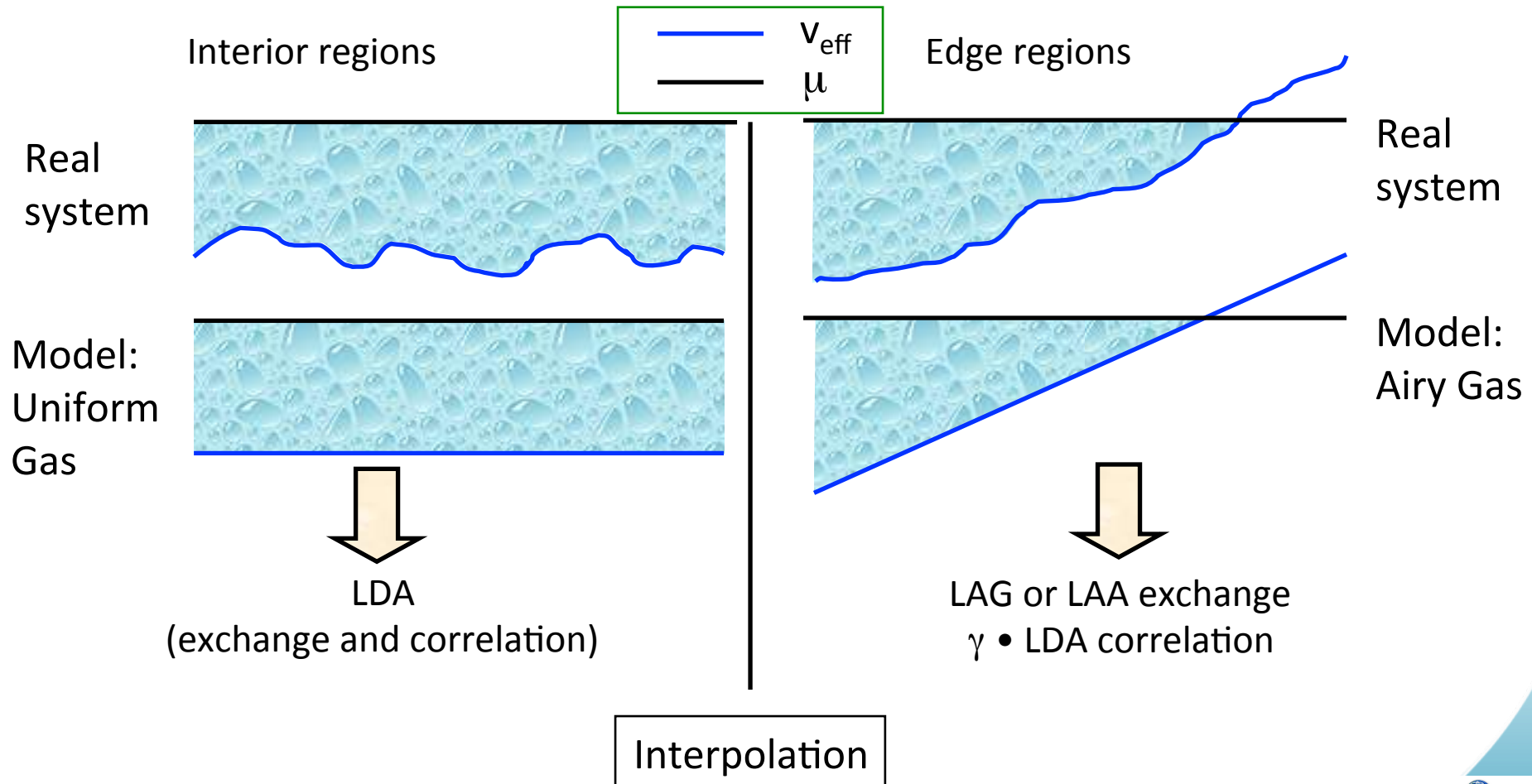
Generalized Idea



Every subsystem functional is designed to capture a specific type of physics, appropriate for a particular subsystem.

General functional from subsystem

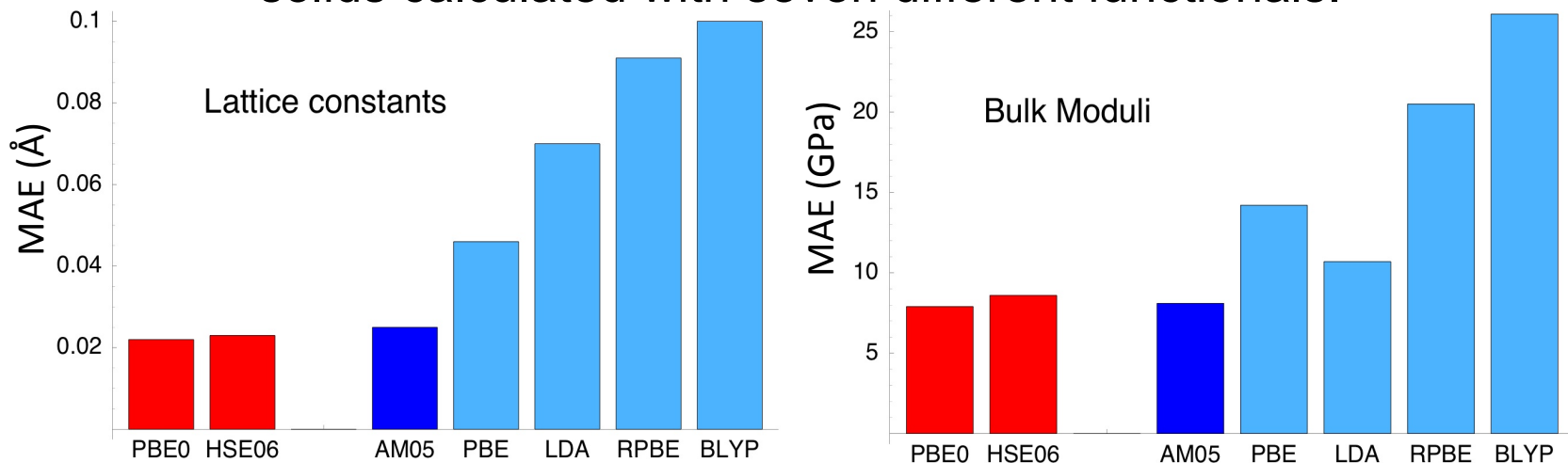
functionals: AM05, PRB 72, 085108 (2005)



Two constants (one is γ above, one is in interpolation index) are determined by fitting to yield correct jellium surface energies.

AM05 is as accurate as a **hybrid**, but much faster

Comparison of mean absolute errors (MAE) for properties of 20 solids calculated with seven different functionals.



JCP 128, 084714 (2008)

GGA type functionals (**blue**) are one to three order of magnitudes faster to use than **hybrids** (**red**). **AM05** has the same accuracy as **hybrids** for solids and thus enable accurate and fast DFT calculations of, for example, defects in semi-conductors. It also allows for the use of DFT-MD as an accurate tool in EOS construction.

AM05 also proves that fast AND accurate is possible.

Side note: Large N vs slowly varying limit

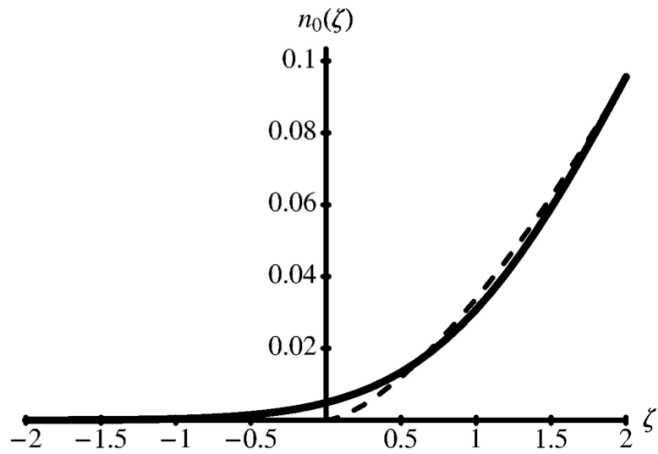


FIG. 5. The density of the Airy gas, exact (solid line) and the Thomas Fermi approximation (dashed line).

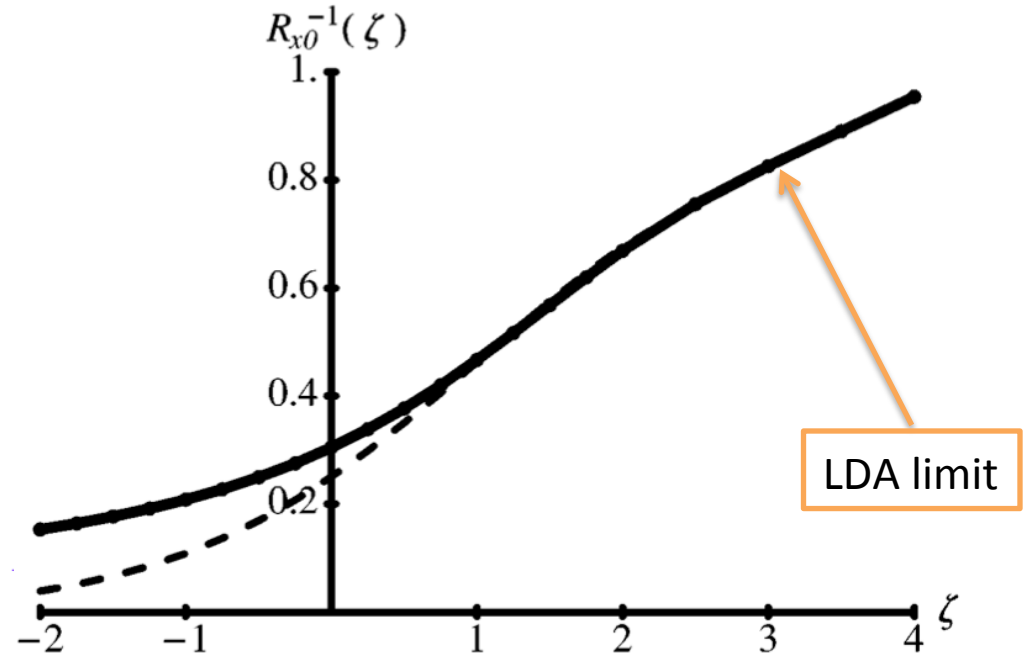


FIG. 6. The inverse radius of the exchange hole of the Airy gas: (solid line) exact, (dashed line) LDA.

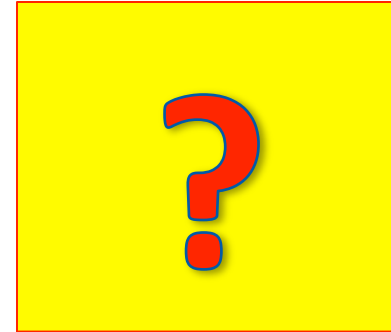
AG goes to large N limit, not slowly varying limit. AG exchange energy does not fulfill gradient expansion for slowly varying density.

Subsystem Functional Scheme:

$$E_{xc} = \int_V n(\vec{r}) \varepsilon_{xc}(\vec{r}; [n]) dV$$

Dividing V into sub-regions where different subsystem functionals apply

Specialized functionals in different subsystems

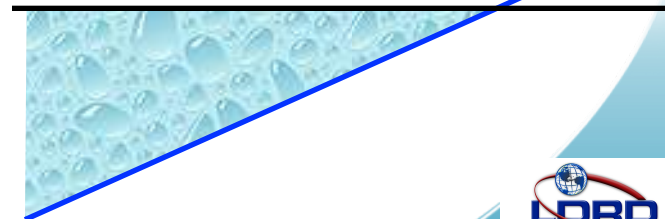


Interior physics:
Uniform electron gas



Interpolation
Index:
ELF

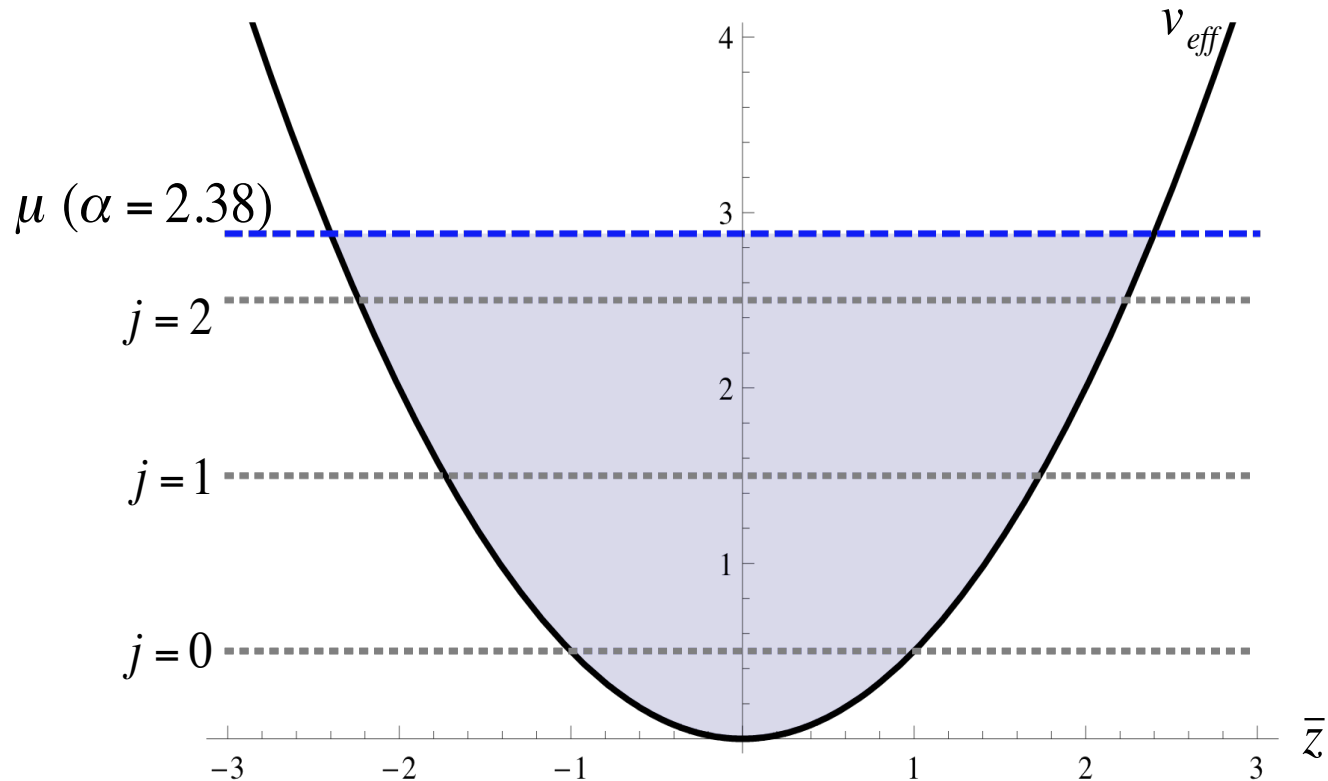
Surface physics:
Airy Gas



Harmonic Oscillator model (HO)

Hao, Armiento and Mattsson Phys, Rev. B **82**, 115103 (2010).

HO model: Localized electron levels in a continuum.

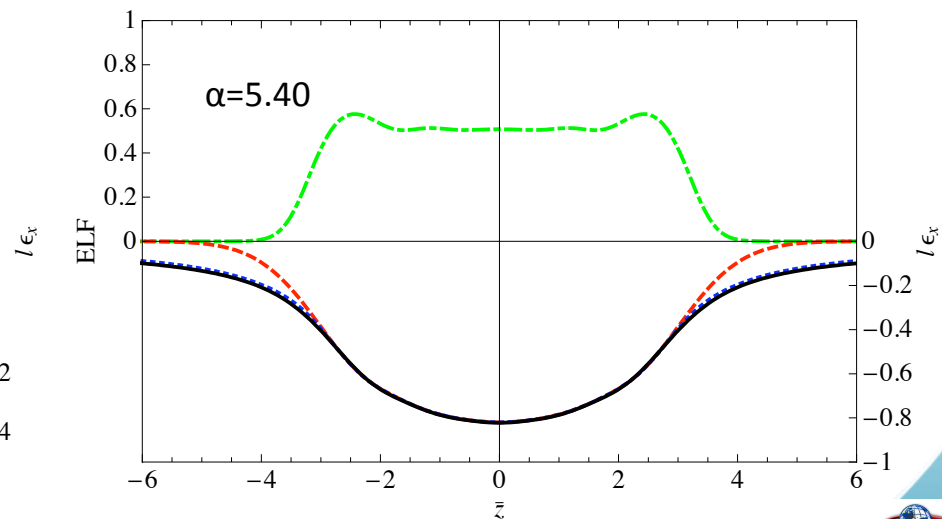
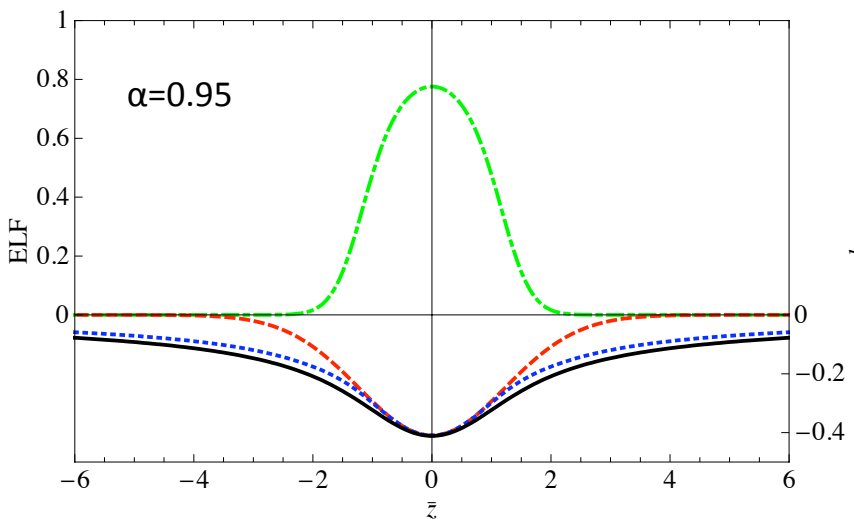
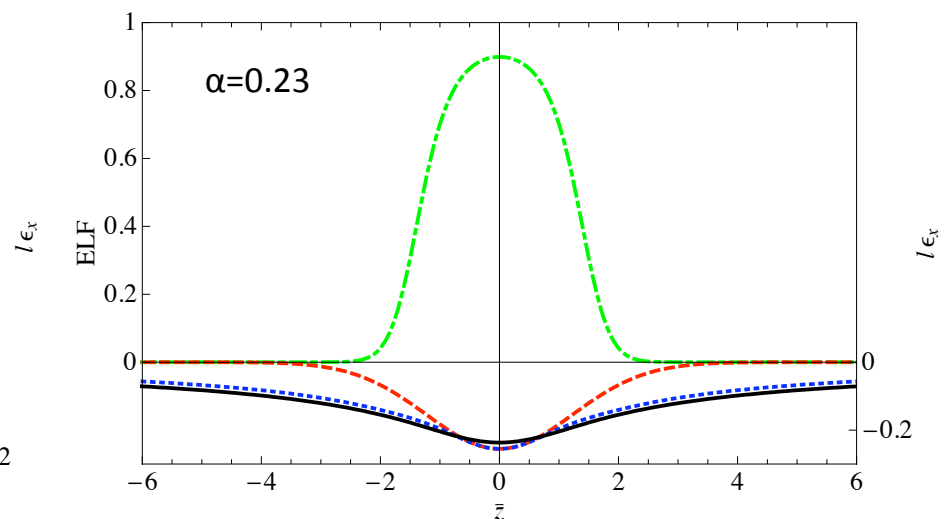
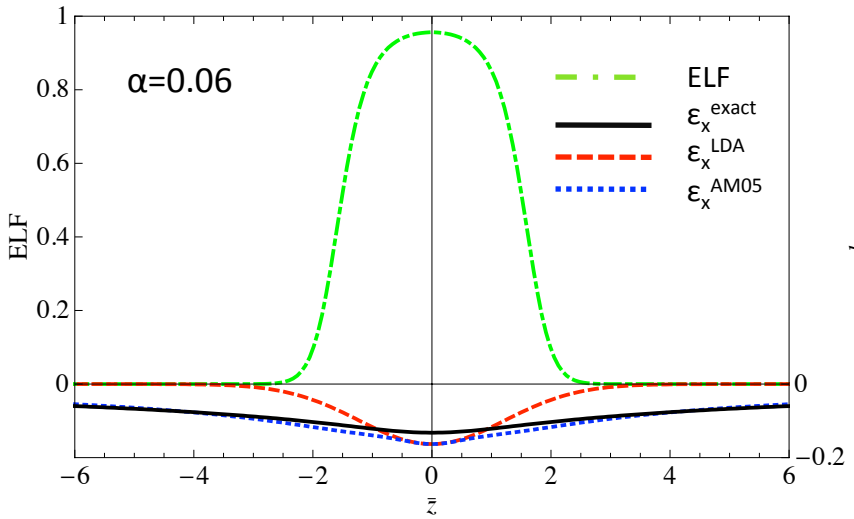


Energy of subbands $\varepsilon_j = \left(j + \frac{1}{2}\right) \frac{1}{l^2}$

Chemical potential $\mu = \left(\alpha + \frac{1}{2}\right) \frac{1}{l^2}$

α characterizes how many subbands have been occupied, and determines the level of confinement.

ELF in HO systems versus Exchange Energy



ELF is correlated with the exchange energy errors!

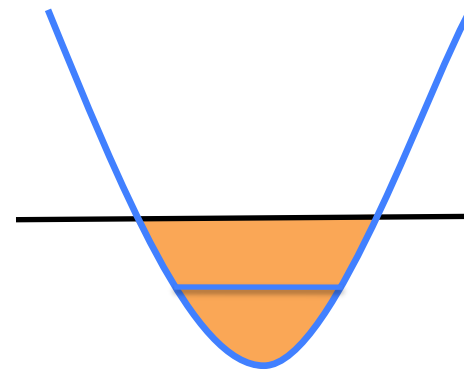
Subsystem Functional Scheme:

$$E_{xc} = \int_V n(\vec{r}) \varepsilon_{xc}(\vec{r};[n]) dV$$

Dividing V into sub-regions where different subsystem functionals apply

Specialized functionals in different subsystems

Confinement physics:
Harmonic oscillator gas

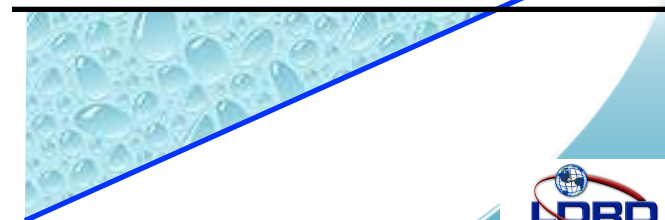


Interior physics:
Uniform electron gas

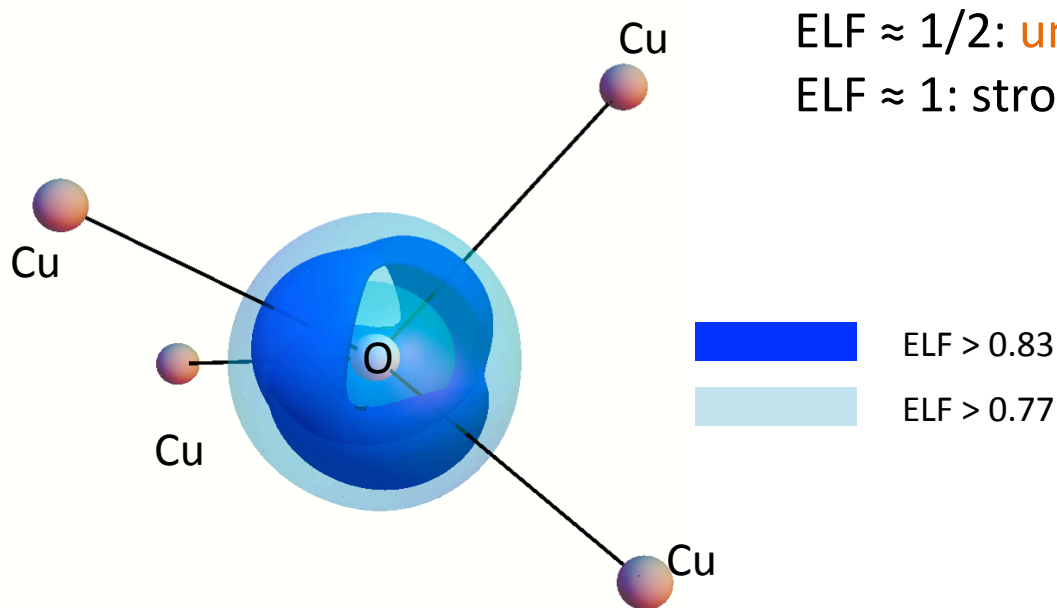


Interpolation
Index:
ELF

Surface physics:
Airy Gas



ELF in a 'real' system: CuO, transition metal oxide



CuO: Monoclinic structure obtained when starting from the experimental structure with each dimension scaled by 3%

The high ELF regions are around the oxygen atoms. We identify these as the regions where hybridization in solid materials occur.

Si from QMC

ANTONIO C. CANCIO AND M. Y. CHOU

PHYSICAL REVIEW B 74, 081202(R) (2006)

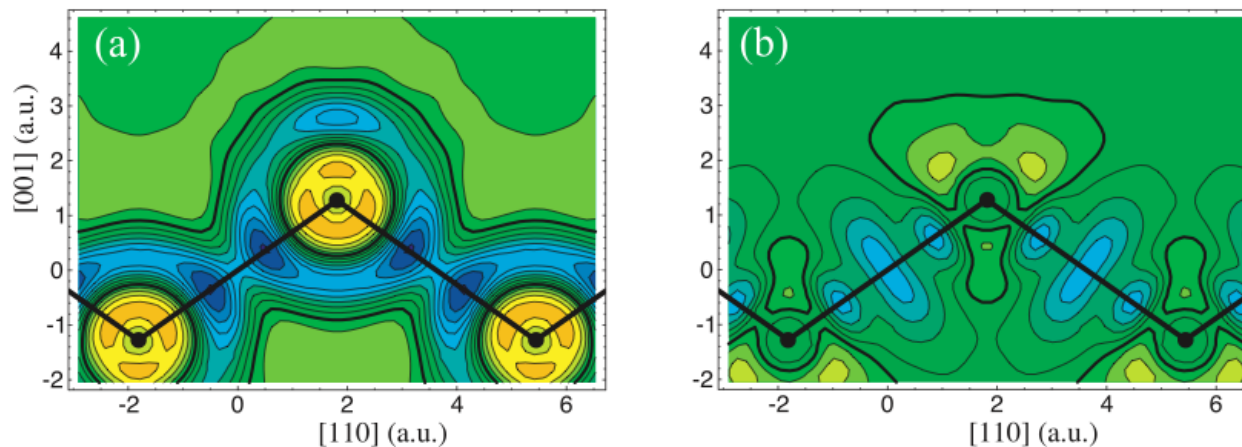
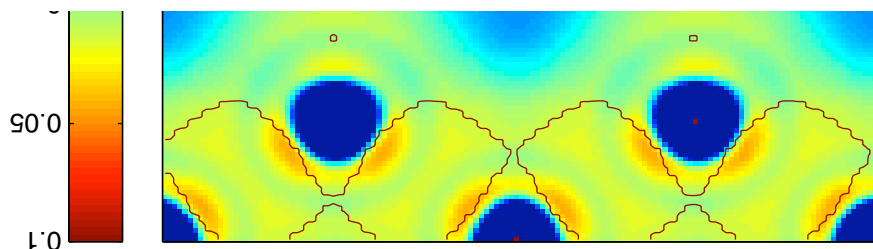


FIG. 1. (Color) Comparison of DFT and VMC e_{xc} 's on the (110) plane of the Si crystal. (a) Difference between the LDA e_{xc} and that of VMC data (Ref. 10). Difference between that of the GGA++ model described in the text and the VMC result. Contours in increments of 0.2×10^{-3} a.u., with thicker contour that for zero difference. Bluer (darker) regions show negative difference and redder (lighter) regions, positive.



Si from QMC

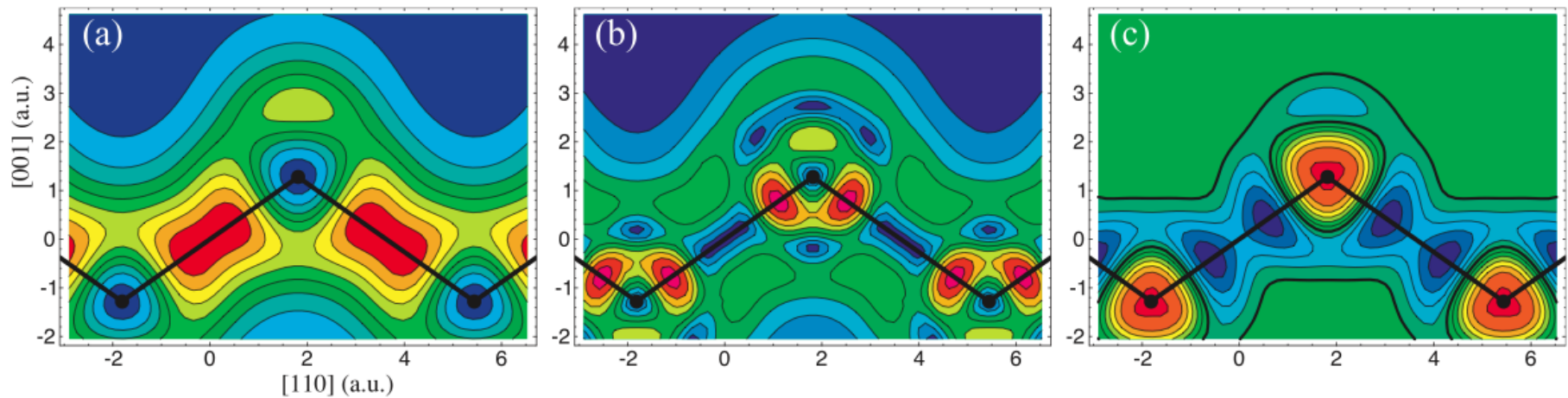
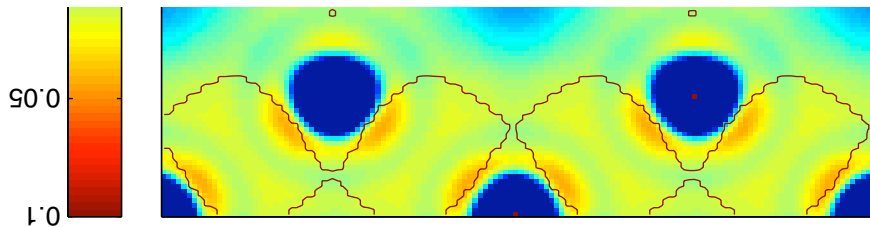


FIG. 2. (Color) Gradient analysis of the density of crystalline Si. The density n (a), $|\nabla n|$ (b), and $\nabla^2 n$ (c) on the (110) plane of the Si crystal. Atoms and bonds outlined in black. Shading varies from blue (dark gray) (low) to red (light gray) (high) and contours are in increments of 0.01 (a), 0.01 (b), and 0.05 a.u. (c). In (c) the zero contour is the thicker black line.



Summary

- The interesting properties of actinide systems comes from a simultaneous existence of **free** and **discrete level** electrons.
- The challenge we have is to describe **free electrons** and **discrete level electrons** equally well in a unified picture.
- The ELF index can be used to find regions in real space where **discrete level physics** needs to be taken into account.
- We have identified the HO gas as a model system that can be used to gain insight about this kind of physics.
- We will use the HO gas model system for creating a functional suitable for these systems via the subsystem functional scheme.

Kinetic energy functionals

$$\left(-\frac{\hbar^2}{2m} \nabla^2 + v_{eff}(\mathbf{r}) \right) \psi_\nu(\mathbf{r}) = \epsilon_\nu \psi_\nu(\mathbf{r}) \quad \nu = 1, 2, \dots, N$$

$$n(\mathbf{r}) = \sum_{\nu=1}^N |\psi_\nu(\mathbf{r})|^2$$

$$v_{eff}(\mathbf{r}) = v(\mathbf{r}) + \int \frac{n(\mathbf{r}')}{|\mathbf{r} - \mathbf{r}'|} d\mathbf{r}' + \frac{\delta E_{xc}[n(\mathbf{r})]}{\delta n(\mathbf{r})}$$

$$E[n] = T_s[n] + E_{ext}[n] + E_{hartree}[n] + E_{xc}[n]$$

Minimize wrt density: $\delta E / \delta n = 0$

Kinetic energy functionals

Calculate the kinetic energy density $\tau = T_s/V$ for a uniform electron gas.
 Calculate the electron density n for a uniform electron gas.

Express T_s as a functional of the density n , $T_s[n]$.

This is the Thomas-Fermi approximation for the kinetic energy.

$$\left. \begin{aligned} \tau_{\text{UEG}} &= k_F^5/5/\pi^2 \\ n_{\text{UEG}} &= k_F^3/3/\pi^2 \end{aligned} \right\} \longrightarrow \tau_{\text{TF}} = 3/5 (3\pi^2)^{2/3} n^{5/3}$$

This is corresponding to LDA for exchange-correlation functionals

Kinetic energy functional for surface system

Calculate the kinetic energy density for a surface system

Calculate the electron density for a surface system

Express T_s as a functional of the density n

This is a surface approximation for the kinetic energy.

We can easily calculate τ for the Airy gas. We have n for an Airy gas.

We need to express τ as a function of n and its derivatives.

Possibly we need to use an interpolation index to interpolate between TF and Airy. Need to remember to use same definition for all subsystems.

Vitos et al have made a parameterization: PRA **61**, 052511 (2000).

This is corresponding to LAA and LAG for exchange functionals.

Kinetic energy functional for confined systems

Calculate the kinetic energy density for a confined system

Calculate the electron density for a confined system

Express T_s as a functional of the density n

This is a confined system approximation for the kinetic energy.

We can easily calculate τ for the Harmonic Oscillator (HO) gas. We have n for a HO gas.

We need to express τ as a function of n and its derivatives.

Possibly we need to use an interpolation index to interpolate between HO, TF, and Airy. Need to remember to use same definition for all subsystems.

Kinetic energy functional for confined systems

$$t = \frac{\tau}{\tau^{unif}} = \frac{\tau}{(3/10)(3\pi^2)^{2/3}n^{5/3}}$$

For a HO system with $\alpha < 1$:

$$t = \frac{5}{3} \frac{\alpha + \bar{z}^2}{(3\pi^{1/2}\alpha e^{-\bar{z}^2})^{2/3}}$$

$$\left\{ \begin{array}{l} s = \frac{|\nabla n|}{2(3\pi^2)^{1/3}n^{4/3}} = \frac{|2\bar{z}|}{2(3\pi^{1/2}\alpha e^{-\bar{z}^2})^{1/3}} \\ q = \frac{\nabla^2 n}{4(3\pi^2)^{2/3}n^{5/3}} = \frac{4\bar{z}^2 - 2}{4(3\pi^{1/2}\alpha e^{-\bar{z}^2})^{2/3}} \end{array} \right.$$

$$\left\{ \begin{array}{l} \alpha = \left[\frac{1}{2(s^2 - q)} \right]^{3/2} / (3\pi^{1/2} e^{-\frac{s^2}{2(s^2 - q)}}) \\ \bar{z}^2 = \frac{s^2}{2(s^2 - q)} \end{array} \right.$$

$$t = \frac{5}{3} \left(\frac{1}{\sqrt{2(s^2 - q)}} \frac{1}{3\pi^{1/2} e^{-\frac{s^2}{2(s^2 - q)}}} + s^2 \right)$$

Not final answer...